*MRS Communications (2013)*, *3*, 67–71
© Materials Research Society, 2013
doi:10.1557/mrc.2013.8

MRS Communications

Research Letters

# Examining the interlayer interactions formed between reduced graphene oxide and ionic liquids

**Natis Shafiq** and **Muge Acik,** Department of Materials Science and Engineering, The University of Texas at Dallas, Richardson, Texas 75080-3021
**Daniel R. Dreyer,** Department of Chemistry and Biochemistry, The University of Texas at Austin, Austin, Texas 78712
**Juan Juarez,** Department of Materials Science and Engineering, The University of Texas at Dallas, Richardson, Texas 75080-3021
**Christopher W. Bielawski,** Department of Chemistry and Biochemistry, The University of Texas at Austin, Austin, Texas 78712
**Yves J. Chabal,** Department of Materials Science and Engineering, The University of Texas at Dallas, Richardson, Texas 75080-3021

Address all correspondence to Yves J. Chabal at **chabal@utdallas.edu**

(Received 15 February 2013; accepted 18 February 2013)

## Abstract

It is important to understand the electrolyte–electrode interactions for fabricating graphene oxide (GO)- and ionic liquid (IL)-based ultracapacitors. Therefore, we explored how the type and size of the cations in various ILs determine the nature of processed materials. In all cases, the ILs intercalate into the graphitic structure but marked differences are observed during exfoliation via thermal reduction. The combination of a long alkyl chain ammonium-based cation and a large-volume anion leads to strong interactions and defect formation, as evidenced by $CO_2$ production during annealing. In contrast, using the same anions but different cations stabilize the GO functional groups below 400 °C.

Substantial improvement in the cycling efficiency of energy storage devices is necessary to increase their overall performance, requiring a focused effort in the development of new nanoscale materials. Recently, ultracapacitors have attracted attention because, in contrast to batteries, they exhibit high power delivery (10 kW/kg) and a long life cycle.[1] Ultracapacitors typically consist of two porous carbon electrodes separated by an ion porous polymer membrane. When a supporting electrolyte is added, an ionic current can flow between the electrodes.[2] The performance of ultracapacitors

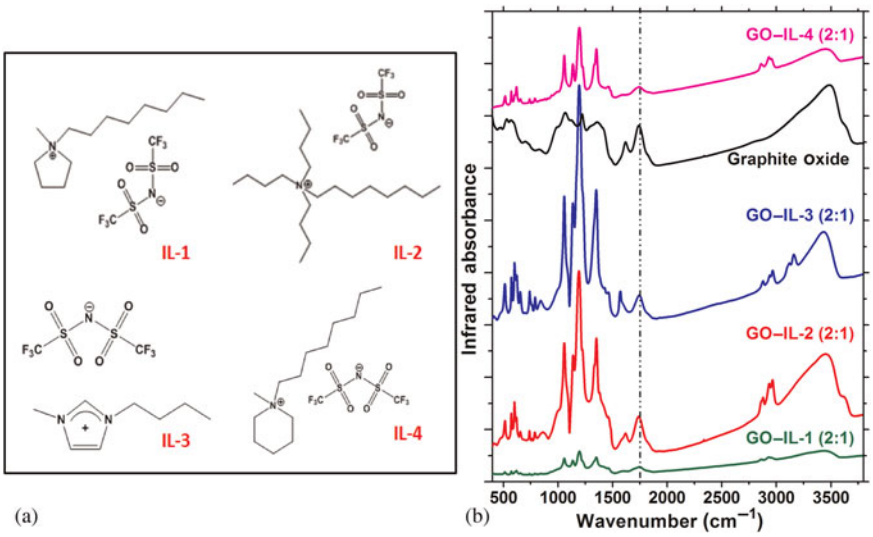



**Figure 1.** (a) Chemical structures of the ILs studied: IL-1 (*N*-methyl-*N*-octylpyrrolidinium bis(trifluoromethanesulfonyl)imide), IL-2 (*N*-octyl-*N*,*N*,*N*-tributylammonium bis(trifluoromethanesulfonyl)imide), IL-3 (1-butyl-3-methylimidazolium bis(trifluoromethanesulfonyl)imide), IL-4 (*N*-octyl-*N*-methylpiperidinium bis(trifluoromethanesulfonyl)imide) and (b) infrared transmission absorbance spectra of GO and GO–IL composites in 2:1 ratios (w/w) prepared in deionized water at room temperature: GO–IL-1, GO–IL-2, GO–IL-3, and GO–IL-4.



https://doi.org/10.1557/mrc.2013.8 Published online by Cambridge University Press

can be improved by using new kinds of electrode materials and electrolytes, such as graphene-based nanomaterials, that possess high intrinsic surface areas and are chemically inert under a wide range of applied potentials.[1] Moreover, the energy density of ultracapacitors increases at higher cell voltages, although increased applied potentials require highly stable electrolytes to avoid decomposition under operating conditions.[3] To this end, ionic liquids (ILs) are now widely explored as electrolytes as they exhibit excellent electrochemical stability, high ionic conductivity, and thermal stability, as well as non-volatility, non-flammability, and low toxicity.[4]

Reduced graphite oxide (RGO) is one of the most commonly used precursors for modified graphene and can be prepared either by chemical reduction or thermal annealing of graphene oxide (GO).[5,6] Indeed, good capacitance values can be achieved using chemically or thermally modified graphene electrodes with either aqueous or organic electrolytes.[4] However, despite the widespread utilization of ILs as electrolytes in graphene-based ultracapacitors, there is still a lack of fundamental understanding of the interactions between the two components. Therefore, it is important to investigate the interlayer interactions in modified graphene–IL composites to

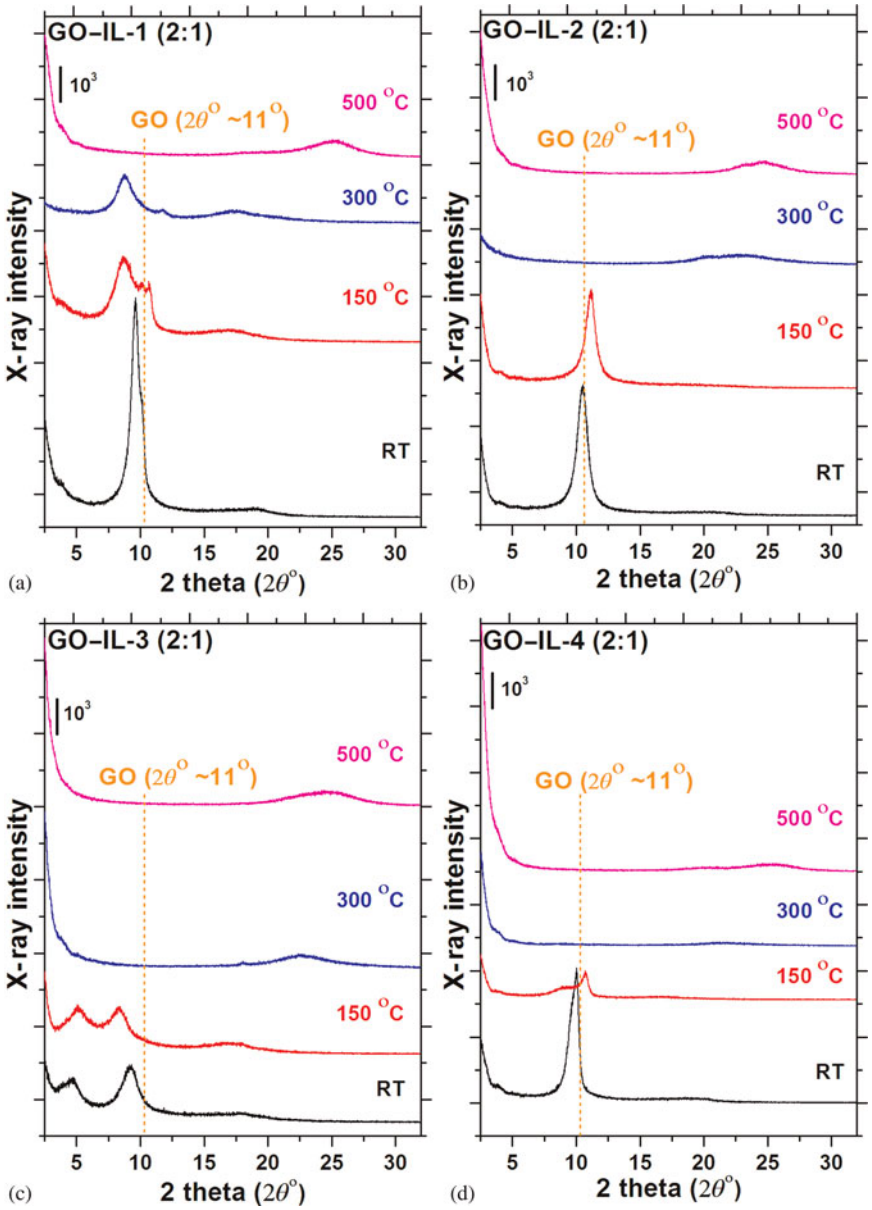



**Figure 2.** X-ray diffraction patterns (XRD) of GO–IL composites for (a) GO–IL-1, (b) GO–IL-2, (c) GO–IL-3, and (d) GO–IL-4 at room temperature, and after annealing at 150, 300, and 500 °C. Orange dashed line indicates XRD pattern of as-synthesized graphite oxide (GO) with a (002) orientation at $2\theta = 11°$, corresponding to an interlayer spacing of approximately 9 Å.


https://doi.org/10.1557/mrc.2013.8 Published online by Cambridge University Press

properly optimize graphene-based ultracapacitors with ILs as electrolytes.

To study the interlayer interactions between RGOs prepared by thermal annealing in the presence of ILs, four different ILs were selected. These ILs were specifically designed to study the role of cations in interlayer interactions. To that end, the same anion was used, namely bis(trifluoromethanesulfonyl)imide [Fig. 1(a)]. GO was synthesized according to the modified Hummers' method[7] and intercalated with each IL at a GO-to-IL (GO–IL) ratio of 2:1 (w/w) in 4 mL of deionized (DI) water by magnetically stirring overnight to prepare a GO–IL composite. X-ray diffraction (XRD) patterns (Fig. 2) of the recovered products indicated that intercalation of each IL took place, as evidenced by a variation of the interlayer distance of the original GO [Figs. 2(a)–2(d)]. The original GO exhibited a $2\theta$ value of 11°, while intercalation of various ILs led to lower values, namely 9.6° for GO–IL-1 [Fig. 2(a)], 10.4° for GO–IL-2 [Fig. 2(b)], 9.2° for GO–IL-3 [Fig. 2(c)], and 10.0° for GO–IL-4 [Fig. 2(d)], confirming that the ILs penetrated into the GO interlayers. GO–IL-3 [Fig. 2(c)] showed the largest shift of all due to the strong interactions between IL-3 and GO (with the smallest molecular volume of 326.85 $Å^3$). The lowest intercalation efficiency was observed for IL-2 [Fig. 2(b)] with an ammonium-based cation and long-chain alkyl substituents, which was attributed to its large molecular volume (553.04 $Å^3$), the largest of the four ILs investigated herein.

To further investigate the interactions between GO and the ILs, a series of Fourier transform infrared (FT-IR) measurements were performed on the starting GO and IL-intercalated GO for each IL. The infrared absorbance spectrum of the as-synthesized GO [black curve in Fig. 1(b)] collected at room temperature is characterized by the vibrational stretch modes of C–O (1000–1200 $cm^{-1}$), C–O–C (1230–1330 $cm^{-1}$), $sp^2$–C (1580–1600 $cm^{-1}$), COOH (1650–1750 $cm^{-1}$), C = O (1750–1850 $cm^{-1}$), and total C–OH at ~3600–3750 $cm^{-1}$. After IL intercalation in the as-synthesized GO, there is a substantial absorption intensity increase of the $sp^3$–C

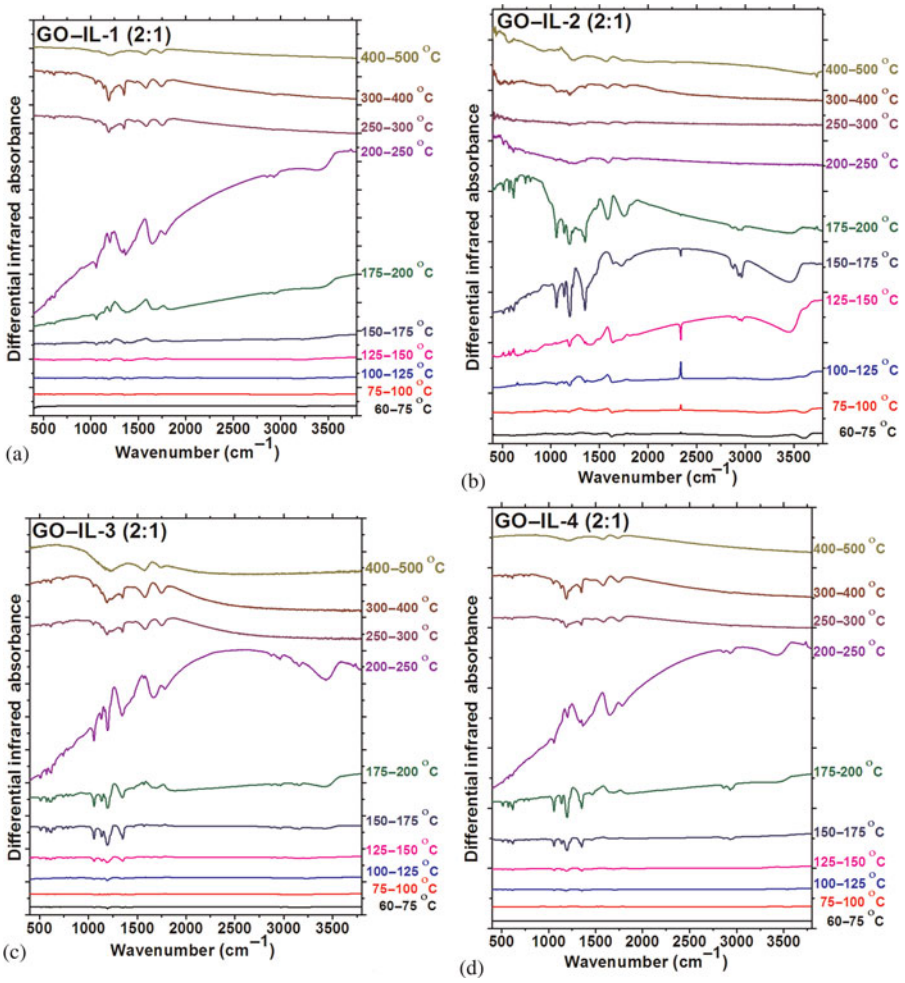



**Figure 3.** Infrared transmission differential spectra of GO–IL (2:1) composites of (a) GO–IL-1, (b) GO–IL-2, (c) GO–IL-3, and (d) GO–IL-4 annealed stepwise in the temperature range of 60–500 °C.



https://doi.org/10.1557/mrc.2013.8 Published online by Cambridge University Press

stretching modes of $CH_2$ and absorption related to the $CH_3$ alkyl groups of the cations in the frequency range of ~1000–1500 $cm^{-1}$ and additional weaker contributions in the ~2800–3000 $cm^{-1}$ range [Fig. 1(b)]. The infrared (IR) data suggest that there is no covalent functionalization of GO by the ILs at room temperature, i.e., GO remains chemically stable.

Next, *in situ* IR analysis was performed on the composites as a function of annealing temperature. The differential spectra in Fig. 3 show the variation in the GO–IL composite structures as a function of annealing temperatures (60–500 °C). Upon annealing to 150–250 °C, there is formation of ketone moieties (C = O) with modes in the ~1100–1400 and ~1500–1850 $cm^{-1}$ ranges, as seen in the spectra of GO–IL-1 [Fig. 3(a)], GO–IL-3 [Fig 3(c)], and GO–IL-4 [Fig. 3(d)], indicative of interactions between water and the defective sites of the RGO graphitic backbone, as discussed in our previous study.[8]

Notably, ketones (C = O) form at lower temperatures (60–150 °C) in the case of GO–IL-2 [Fig. 3(b)] compared with other GO–IL composites. This experimental finding indicates that water is not completely replaced by IL in the interlayer when GO is exposed to IL-2 under the conditions explored. This indicates that IL-2, composed of a bulky and highly substituted ammonium-based cation [Fig. 1(a)], cannot fully displace water from the interlayer of GO during the intercalation process, whereas other ILs can to a greater extent. In fact, the evolution of $CO_2$ [~2300 $cm^{-1}$ in Figs. 3(b) and 4(b)] is observed during annealing in the presence of trapped water in the interlayer spacing of GO–IL-2, believed to be a result of defect formation in RGO, and can indirectly be used to determine the presence of water in GO. $CO_2$ formation was not observed upon annealing GO–IL-1 [Fig. 3(a)], GO–IL-3 [Fig. 3(c)], or GO–IL-4 [Fig. 3(d)], indicating that defects did not form in these composites, thus confirming the prior removal

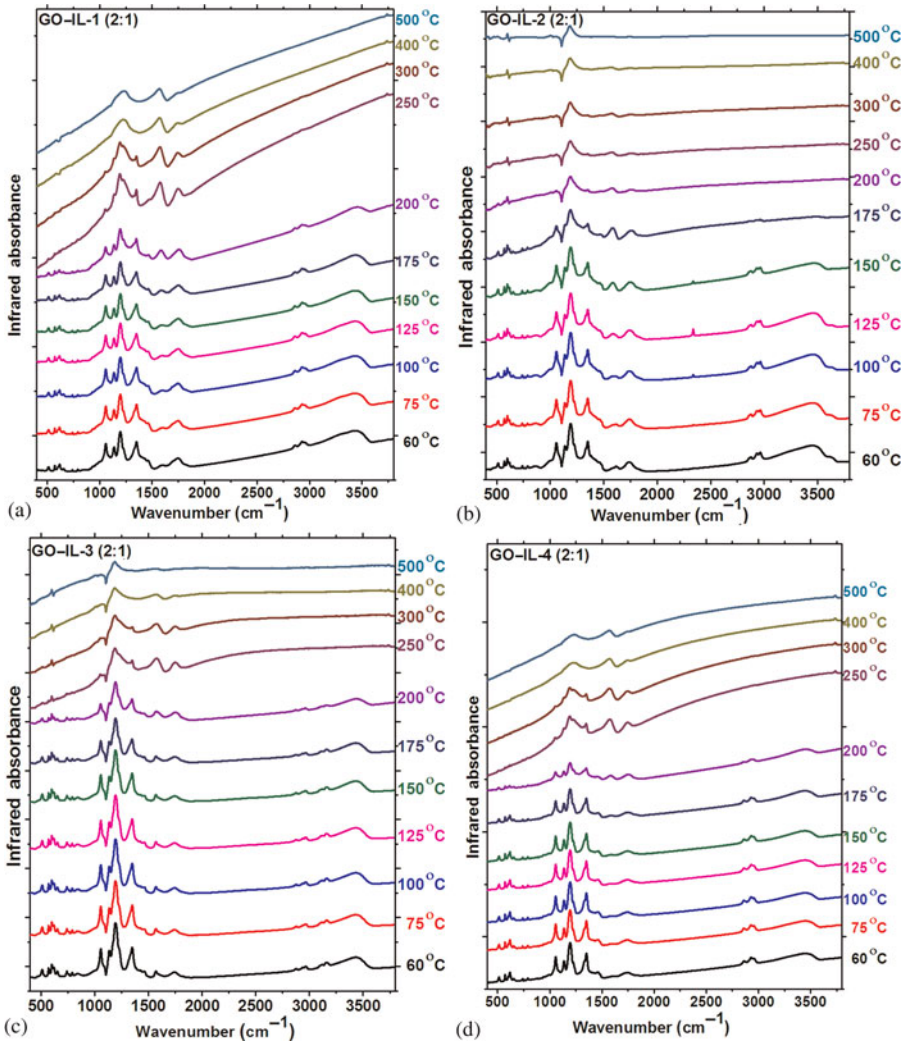



**Figure 4.** Infrared transmission absorbance spectra of GO-IL (2:1) composites of (a) GO–IL-1, (b) GO–IL-2, (c) GO–IL-3, and (d) GO–IL-4 annealed stepwise in a temperature regime of 60–500 °C.


https://doi.org/10.1557/mrc.2013.8 Published online by Cambridge University Press

of water during IL insertion. In contrast, $CO_2$ was produced when GO–IL-2 was annealed at 60–100 °C, and was then consumed at 125–175 °C [Figs. 3(b) and 4(b)]. This experimental finding showed that water, initially present in the case of GO–IL-2, was not removed and could therefore react with the graphitic backbone, generating defects similarly to what occurs in pure GO. However, the trapped water was then removed after annealing at 125 °C, as evidence by a sharp decrease in $CO_2$ formation [Fig. 3(b)]. Although IL-1, IL-3, and IL-4 do not develop defects similar to IL-2, they induce a large expansion of the reduced GO layers. In particular, IL-1 and IL-3 expand the GO layers upon annealing at 150 and 300 °C [Figs. 2(a) and 2(c)]. In contrast, GO–IL-2 does not expand RGO, as evidenced by a small $2\theta$ shift in the XRD patterns after annealing at 150 °C [Fig. 2(b)].

Overall, the stability of GO functional groups is strongly dependent on the interlayer interactions of RGO with ILs during annealing. For instance, IL-1 promotes the removal of GO oxygen groups when the intercalation compounds are annealed at temperatures up to 400 °C. In addition, hydroxyl desorption is observed at annealing temperatures of 150–250, 60–200, 175–250, and 175–250 °C for GO–IL-1, GO–IL-2, GO–IL-3, and GO–IL-4, respectively [Figs. 3(a) and 3(d)]. These results indicate that the stability of OH groups is significantly decreased as the water molecules are removed from the interlayer, compared with when water remains trapped without ILs in the interlayer. When ILs are absent from the interlayer (i.e., as-synthesized GO), hydroxyls remain thermally stable up to an annealing temperature of 300 °C.[9]

In summary, we have investigated the interlayer interactions in GO–IL composites prepared from GO and several ILs composed of a common anion (bis(trifluoromethanesulfonyl)imide) and one of several cations intercalated into the GO interlayer spacing. Bulky ILs cannot be efficiently intercalated due to their large size. Experimental findings from in situ infrared spectroscopy combined with XRD studies show that IL with bulky and highly substituted ammonium-based cations (IL-2) promotes defect formation in the graphitic basal plane during annealing at 60–500 °C. In addition, imidazolium- and pyrrolidinium-based ILs (IL-1 and IL-3) promote strong interlayer interactions that minimize the expansion of RGO layers. Differential IR spectra also confirmed that these cations stabilize the GO oxygen functional groups during thermal annealing, with minimal decomposition at temperatures up to 400 °C.

## Acknowledgments

The authors acknowledge the full financial support of the U.S. Department of Energy, Office of Basic Energy Sciences, Division of Materials Sciences and Engineering under Award DE-SC001951.

## References

1. S. Park and R.S. Ruoff: Chemical methods for the production of graphenes. *Nat. Nanotechnol.* **4**, 217 (2009).
2. M.D. Stoller, S. Park, Y. Zhu, J. An, and R.S. Ruoff: Graphene-based ultracapacitors. *Nano Lett.* **8**, 3498 (2008).
3. P. Simon and Y. Gogotsi: Materials for electrochemical capacitors. *Nat. Mater.* **7**, 845 (2008).
4. C. Liu, Z. Yu, D. Neff, A. Zhamu, and B.Z. Jang: Graphene-based supercapacitor with an ultrahigh energy density. *Nano Lett.* **10**, 4863 (2010).
5. K. Zhang, L. Mao, L.L. Zhang, H.S.O. Chan, X.S. Zhao, and J. Wu: Surfactant-intercalated, chemically reduced graphene oxide for high performance supercapacitor electrodes. *J. Mater. Chem.* **21**, 7302 (2011).
6. D.R. Dreyer, S. Park, C.W. Bielawski, and R.S. Ruoff: The chemistry of graphene oxide. *Chem. Soc. Rev.* **39**, 228 (2010).
7. S. Gilje, S. Han, M. Wang, K.L. Wang, and R.B. Kaner: A chemical route to graphene for device applications. *Nano Lett.* **7**, 3394 (2007).
8. M. Acik, C. Mattevi, C. Gong, G. Lee, K. Cho, M. Chhowalla, and Y. J. Chabal: The role of intercalated water in multilayered graphene oxide. *ACS Nano* **4**, 5861 (2010).
9. M. Acik, G. Lee, C. Mattevi, A. Pirkle, R.M. Wallace, M. Chhowalla, K. Cho, and Y.J. Chabal: The role of oxygen during thermal reduction of graphene oxide studied by infrared absorption spectroscopy. *J. Phys. Chem. C* **115**, 19761 (2011).



https://doi.org/10.1557/mrc.2013.8 Published online by Cambridge University Press